Topological magnon modes of a chain of magnetic spheres in a waveguide

Faezeh Pirmoradian,[1] MirFaez Miri,[2] Babak Zare Rameshti,[1,*] and Shahpoor Saeidian[3]
[1]*Department of Physics, Iran University of Science and Technology, Narmak, Tehran 16846-13114, Iran*
[2]*Department of Physics, University of Tehran, P. O. Box 14395-547, Tehran, Iran*
[3]*Department of Physics, Institute for Advanced Studies in Basic Sciences (IASBS), Zanjan 45137-66731, Iran*

(Received 8 October 2021; revised 23 January 2023; accepted 24 January 2023; published 1 February 2023)

We study topological features of a bipartite chain of magnetic spheres embedded in a rectangular metallic waveguide. The coherently coupled chain via the waveguide mode can host two topologically distinct phases identified by the Zak phase. A finite chain supports a pair of doubly degenerate topological edge states within the gap when the intercoupling dominates over the intracoupling, demonstrating that despite the strong coupling to the waveguide mode, the bulk-edge correspondence still holds. The nontrivial (trivial) topological phase is determined by the intracell and intercell coupling of magnetic spheres which depend on the separation, the external magnetic inductions, and the waveguide dimensions. *Magnetically tunable* topological magnon modes may enable unprecedented topological photonic devices.

DOI: 10.1103/PhysRevB.107.064401

I. INTRODUCTION

A controllable hybrid light-matter system is appealing for storage, communication, and processing of quantum information. Spin ensembles strongly coupled to microwave photons, where the coupling rate exceeds the loss rates, offer a versatile platform to test the fundamental physics and novel applications [1–4]. Magnons, the quanta of collective excitation in the ordered magnetic system, can couple strongly to microwave cavity photons resulting in a hybridized state (magnon polariton) which offers synergistic properties beyond the attractive features of magnons and photons [5–9]. The coupling of magnons to microwave photons provides a robust quantum bus and triggers a long-range coupling between a variety of matter systems, which is mostly of coherent nature in closed cavities [10–12] while of dissipative nature in open cavities and waveguides [13,14].

Harnessing the topologically nontrivial features of collective excitations provides a way to control hybrid light-matter systems: The photonic analogous of integer quantum Hall effect with a built-in protection that hosts chiral states propagating along the edge of a two-dimensional magneto-optical photonic crystal has been predicted [15] and demonstrated experimentally [16]. Zeeman-splitted exciton-polariton lattices have been proposed to realize Chern insulators [17–20]. A particle-hole-symmetric magnetoplasmon has been predicted to have topological properties reminiscent of a two-dimensional topological superconductor [21]. The photonic quantum spin Hall effect has also been achieved utilizing various hybrid light-matter systems [22–31]. Dynamical tuning of the properties of the optical and microwave resonators, which realizes an artificial magnetic field, has opened a new route to achieve topological nontrivial phases in hybrid systems [32–35].

The bosonic counterpart of Su-Schrieffer-Heeger (SSH) model, which is dedicated to explaining the electronic transport of polyacetylene [36], has been proposed in a variety of systems. The realization of nontrivial topological states along with the localized end states are demonstrated in one-dimensional photonic crystals [37–41], a chain of dielectric [42–44], and plasmonic [45–49] nanoparticles, and also in an array of optical [50,51], and plasmonic [52,53] waveguides coupled by their evanescent fields. The coupled micropillar cavities with topologically protected polaritonic end states [54,55] allow to manipulate the subwavelength electromagnetic localized states. The SSH model has also been suggested in cold atoms in one-dimensional optical lattices [56], phononic crystal waveguide [57,58], and a *chain of magnetic spheres* embedded in the free space [59].

In this paper, we study a bipartite chain of magnetic spheres without direct interaction *inside a rectangular metallic waveguide* (see Fig. 1). The magnetic spheres are subjected to external static magnetic inductions which are either perpendicular or parallel to the chain axis. The coupling to the confined electromagnetic modes of the waveguide coherently couple the magnetic spheres. In the dispersive regime, where the waveguide mode is detuned from the magnonic one, the system can be mapped into a coupled magnetic chain. Due to the boundary conditions imposed by the metallic walls of the waveguide, the photon-mediated interaction of magnetic spheres in unbounded and bounded spaces are distinct. The retardation effect due to the finite light velocity also plays a role. The coupled chain of magnetic spheres, depending on the dimerization strength, can host *two* topologically distinct *gapped* phases, distinguished by the Zak phase [59], regardless of whether the static magnetic inductions are applied along or perpendicular to the chain. Topologically nontrivial (trivial) gapped phase can be achieved by changing the intracell and intercell coupling which depend on the position of the magnetic spheres, the static magnetic inductions, and the waveguide dimensions. The topological phase transition

*bzarer@iust.ac.ir

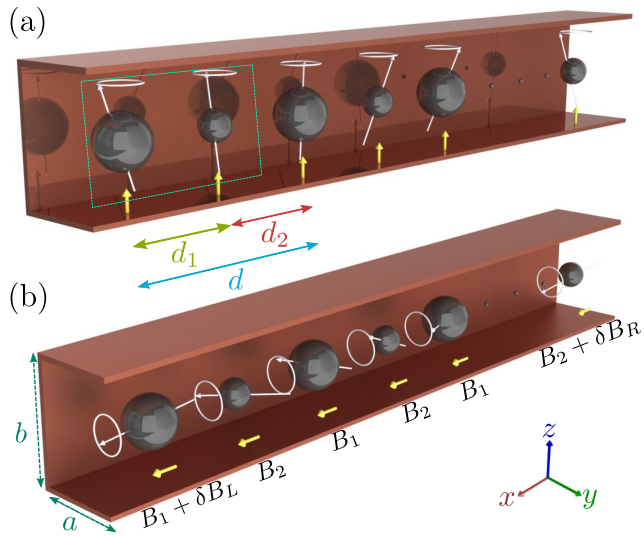

FIG. 1. A bipartite chain of magnetic spheres with N unit cells inside a rectangular microwave waveguide with transverse dimensions a and b. Each unit cell contains two magnetic spheres of macrospins S_1 and S_2. The intracell and intercell separation between neighboring spheres are d_1 and d_2, respectively. Each S_1- (S_2-) type sphere is subjected to a static magnetic induction $\mathbf{B}_1$ ($\mathbf{B}_2$) which is (a) perpendicular and (b) parallel to the axis of the chain. The outermost left and right spheres experience additional magnetic inductions $\boldsymbol{\delta}\mathbf{B}_L$ and $\boldsymbol{\delta}\mathbf{B}_R$, respectively.

goes along with the closing and reopening of the energy gap. A finite chain supports a pair of doubly degenerate topological edge states within the gap when the intracoupling is smaller than the intercoupling confirming the so-called bulk-edge correspondence in the system.

This paper is organized as follows: In Sec. II we present the Hamiltonian of a chain of magnetic spheres inside a microwave waveguide. In Sec. III, we discuss the photon-mediated interaction of two magnetic spheres. The topological properties of the magnonic band structure and the formation of localized edge states in a finite chain of magnetic spheres are addressed in Sec. IV. In Sec. V we conclude and summarize our findings.

II. MODEL

We consider a one-dimensional bipartite chain of magnetic spheres embedded in a long waveguide (see Fig. 1). The chain is composed of N unit cells. The unit cell of the chain consists of two spheres of macrospins S_1 and S_2. The intracell and intercell separations between neighboring spheres are d_1 and d_2, respectively. The nth S_1-type and S_2-type magnetic spheres reside at $\mathbf{r}_n = (nd - d_1/2, y_s, z_s)$ and $\mathbf{r}'_n = (nd + d_1/2, y_s, z_s)$, respectively, where $d = d_1 + d_2$ denotes the lattice constant. Without loss of generality, we assume that the magnetic spheres are in the midplane $z_s = 0$. We consider a hollow rectangular waveguide with perfectly conducting walls located at $y = \pm a/2$ and $z = \pm b/2$. Indeed, $a, b \ll l$ where l denotes the length of the waveguide. The magnetic spheres are assumed to be small compared with the photon wavelength such that only the Kittel mode, i.e., the uniform precession of the magnetization, couples to the waveguide mode.

In the following, we present the Hamiltonians H_m, H_{em}, and H_{int} for the magnetic spheres, the waveguide fields, and the Zeeman interaction of magnetic spheres with the waveguide fields, respectively.

A. Zeeman interaction of magnetic spheres with the static magnetic inductions

We assume that the nth unit cell accommodates two different magnetic spheres with macrospins $\hat{\mathbf{S}}_n = (\hat{S}_n^x, \hat{S}_n^y, \hat{S}_n^z)$ and $\hat{\mathbf{S}}'_n = (\hat{S}_n'^x, \hat{S}_n'^y, \hat{S}_n'^z)$. The magnitudes of macrospins at equivalent sites of the chain are the same, that is, $\hat{\mathbf{S}}_n^2 = S_1(S_1+1)\hbar^2$ and $\hat{\mathbf{S}}_n'^2 = S_2(S_2+1)\hbar^2$. Each S_1- (S_2-) type magnetic sphere experiences a static magnetic induction $\mathbf{B}_1$ ($\mathbf{B}_2$). Moreover, the outermost left (right) sphere is subjected to an additional static magnetic induction $\boldsymbol{\delta}\mathbf{B}_L$ ($\boldsymbol{\delta}\mathbf{B}_R$). The additional magnetic inductions strikingly influence the edge states of the magnetic chain [59]. We study two cases, where the external magnetic inductions are (i) perpendicular and (ii) parallel to the unit vector $\mathbf{n} = \mathbf{e}_x$ along the chain axis.

The Hamiltonian

$$H_m = -\mu \sum_{n=1}^{N} \mathbf{B}_1 \cdot \hat{\mathbf{S}}_n - \mu \sum_{n=1}^{N} \mathbf{B}_2 \cdot \hat{\mathbf{S}}'_n \tag{1}$$

describes the Zeeman interaction of magnetic spheres with the static magnetic inductions. Here $\mu = g\mu_B/\hbar$ is introduced via the g factor g and the Bohr magneton μ_B.

First, we consider the case of $\mathbf{B}_{1,2} = B_{1,2}\mathbf{e}_z$ and $\boldsymbol{\delta}\mathbf{B}_{L,R} = \delta B_{L,R}\mathbf{e}_z$. In the ground state of the magnetic chain, all macrospins point in the direction determined by the external magnetic induction. At low temperatures, however, thermal fluctuations play a decisive role: macrospins slightly deviate from the ground-state direction. To study the low-energy collective excitations of the magnetic chain, we use the Holstein-Primakoff transformation to write the spin operator $\hat{\mathbf{S}}$ ($\hat{\mathbf{S}}'$) in terms of the bosonic operator $\hat{\mathbf{a}}$ ($\hat{\mathbf{b}}$) as

$$\begin{aligned} \hat{S}^+ &= \hbar\sqrt{2S_1}\hat{\mathbf{a}}, \quad \hat{S}'^+ = \hbar\sqrt{2S_2}\hat{\mathbf{b}}, \\ \hat{S}^- &= \hbar\sqrt{2S_1}\hat{\mathbf{a}}^\dagger, \quad \hat{S}'^- = \hbar\sqrt{2S_2}\hat{\mathbf{b}}^\dagger, \\ \hat{S}^z &= \hbar(S_1 - \hat{\mathbf{a}}^\dagger\hat{\mathbf{a}}), \quad \hat{S}'^z = \hbar(S_2 - \hat{\mathbf{b}}^\dagger\hat{\mathbf{b}}). \end{aligned} \tag{2}$$

Here $\hat{S}^\pm = \hat{S}^x \pm i\hat{S}^y$ and $\hat{S}'^\pm = \hat{S}'^x \pm i\hat{S}'^y$. Second, we consider the case of $\mathbf{B}_{1,2} = B_{1,2}\mathbf{e}_x$ and $\boldsymbol{\delta}\mathbf{B}_{L,R} = \delta B_{L,R}\mathbf{e}_x$. We employ the Holstein-Primakoff transformation

$$\begin{aligned} \hat{S}^+ &= \hbar\sqrt{2S_1}\hat{\mathbf{a}}, \quad \hat{S}'^+ = \hbar\sqrt{2S_2}\hat{\mathbf{b}}, \\ \hat{S}^- &= \hbar\sqrt{2S_1}\hat{\mathbf{a}}^\dagger, \quad \hat{S}'^- = \hbar\sqrt{2S_2}\hat{\mathbf{b}}^\dagger, \\ \hat{S}^x &= \hbar(S_1 - \hat{\mathbf{a}}^\dagger\hat{\mathbf{a}}), \quad \hat{S}'^x = \hbar(S_2 - \hat{\mathbf{b}}^\dagger\hat{\mathbf{b}}), \end{aligned} \tag{3}$$

with $\hat{S}^\pm = \hat{S}^y \pm i\hat{S}^z$ and $\hat{S}'^\pm = \hat{S}'^y \pm i\hat{S}'^z$. The magnetic Hamiltonian in both cases can be rewritten as

$$H_m = \hbar\mu B_1 \sum_{n=1}^{N} \hat{\mathbf{a}}_n^\dagger\hat{\mathbf{a}}_n + \hbar\mu B_2 \sum_{n=1}^{N} \hat{\mathbf{b}}_n^\dagger\hat{\mathbf{b}}_n. \tag{4}$$

B. Quantized electromagnetic fields inside a rectangular waveguide

The electromagnetic fields inside a waveguide obey the Maxwell equations and the constitutive equations $\mathbf{D}(\mathbf{r},t)=\epsilon_0\mathbf{E}(\mathbf{r},t)$ and $\mathbf{B}(\mathbf{r},t)=\mu_0\mathbf{H}(\mathbf{r},t)$. It is known that the electromagnetic fields can be written in terms of a vector potential $\mathbf{A}(\mathbf{r},t)$ which obeys the wave equation $\nabla^2\mathbf{A}(\mathbf{r},t)-\frac{1}{c^2}\frac{\partial^2\mathbf{A}(\mathbf{r},t)}{\partial t^2}=0$ and the Coulomb gauge condition $\boldsymbol{\nabla}\cdot\mathbf{A}(\mathbf{r},t)=0$. The vector potential can be expanded in terms of the spatial mode functions $\mathbf{u}_{\mathbf{q},\lambda}(\mathbf{r})$ as

$$\mathbf{A}(\mathbf{r},t)=\sum_{\mathbf{q}}\sum_{\lambda=1,2}\sqrt{\frac{1}{\epsilon_0}}Q_{\mathbf{q},\lambda}(t)\mathbf{u}_{\mathbf{q},\lambda}(\mathbf{r}), \tag{5}$$

where $\mathbf{q}$ and $\lambda=1,2$ denote the wave vector and the mode polarization, respectively. The function $Q_{\mathbf{q},\lambda}(t)$ and the divergenceless vector $\mathbf{u}_{\mathbf{q},\lambda}(\mathbf{r})$ satisfy the equations

$$\frac{\partial^2 Q_{\mathbf{q},\lambda}(t)}{\partial t^2}+\omega_{\mathbf{q}}^2 Q_{\mathbf{q},\lambda}(t)=0, \tag{6}$$

$$\nabla^2\mathbf{u}_{\mathbf{q},\lambda}(\mathbf{r})+\frac{\omega_{\mathbf{q}}^2}{c^2}\mathbf{u}_{\mathbf{q},\lambda}(\mathbf{r})=0. \tag{7}$$

$\mathbf{A}(\mathbf{r},t)$ is real, thus, $Q_{-\mathbf{q},\lambda}(t)=Q^*_{\mathbf{q},\lambda}(t)$, $\omega_{-\mathbf{q}}=\omega_{\mathbf{q}}$, and the solution of Eq. (6) is $Q_{\mathbf{q},\lambda}(t)=\mathrm{Q}_{\mathbf{q},\lambda}e^{-i\omega_{\mathbf{q}}t}+\mathrm{Q}^*_{-\mathbf{q},\lambda}e^{i\omega_{\mathbf{q}}t}$ where $\mathrm{Q}_{\mathbf{q},\lambda}$ is a complex number. On the other hand, $\mathbf{u}_{-\mathbf{q},\lambda}(\mathbf{r})=\mathbf{u}^*_{\mathbf{q},\lambda}(\mathbf{r})$. Moreover, the tangential component of the electric field vanishes on the metallic walls, that is $\mathbf{u}_{\mathbf{q},\lambda}(x,y=\pm\frac{a}{2},z)\cdot\mathbf{e}_z=0$ and $\mathbf{u}_{\mathbf{q},\lambda}(x,y,z=\pm\frac{b}{2})\cdot\mathbf{e}_y=0$. We utilize the following spatial mode functions:

$$\begin{aligned}
\mathbf{u}_{\mathbf{q},1}(\mathbf{r})=&\frac{2}{\sqrt{ab}}\frac{c}{\Omega_{m,m'}}e^{iqx}\left[\frac{m'\pi}{b}\cos\left(\frac{m\pi}{a}y\right)\sin\left(\frac{m'\pi}{b}z\right)\mathbf{e}_y\right.\\
&\left.-\frac{m\pi}{a}\sin\left(\frac{m\pi}{a}y\right)\cos\left(\frac{m'\pi}{b}z\right)\mathbf{e}_z\right],\\
\mathbf{u}_{\mathbf{q},2}(\mathbf{r})=&\frac{2}{\sqrt{ab}}\frac{c^2}{\Omega_{m,m'}}\frac{|q|}{\omega_{\mathbf{q}}}e^{iqx}\\
&\times\left[-\frac{i}{q}\frac{\Omega^2_{m,m'}}{c^2}\sin\left(\frac{m\pi}{a}y\right)\sin\left(\frac{m'\pi}{b}z\right)\mathbf{e}_x\right.\\
&+\frac{m\pi}{a}\cos\left(\frac{m\pi}{a}y\right)\sin\left(\frac{m'\pi}{b}z\right)\mathbf{e}_y\\
&\left.+\frac{m'\pi}{b}\sin\left(\frac{m\pi}{a}y\right)\cos\left(\frac{m'\pi}{b}z\right)\mathbf{e}_z\right],
\end{aligned} \tag{8}$$

where $\mathbf{q}=(q,\frac{m\pi}{a},\frac{m'\pi}{b})$, $m,m'=0,2,4,\ldots,$ $\Omega_{m,m'}=c\sqrt{(\frac{m\pi}{a})^2+(\frac{m'\pi}{b})^2}$, and the photon dispersion relation is $\omega_{\mathbf{q}}=\sqrt{c^2q^2+\Omega^2_{m,m'}}$. Indeed, transverse electric (TE) and transverse magnetic (TM) waves propagating in the waveguide can be expressed in terms of $\mathbf{u}_{\mathbf{q},1}(\mathbf{r})$ and $\mathbf{u}_{\mathbf{q},2}(\mathbf{r})$ mode functions, respectively. The mode functions $\mathbf{u}_{\mathbf{q},\lambda}(\mathbf{r})$ form an orthonormal set:

$$\begin{aligned}
&\int dV\,\boldsymbol{\nabla}\times\mathbf{u}_{\mathbf{q},\lambda}(\mathbf{r})\cdot\boldsymbol{\nabla}\times\mathbf{u}^*_{\mathbf{q}',\lambda'}(\mathbf{r})=l\frac{\omega_{\mathbf{q}}^2}{c^2}\delta_{m,n}\delta_{m',n'}\delta_{q,q'}\delta_{\lambda,\lambda'},\\
&\int dV\,\mathbf{u}_{\mathbf{q},\lambda}(\mathbf{r})\cdot\mathbf{u}^*_{\mathbf{q}',\lambda'}(\mathbf{r})=l\delta_{m,n}\delta_{m',n'}\delta_{q,q'}\delta_{\lambda,\lambda'}.
\end{aligned} \tag{9}$$

Now the Lagrangian of the electromagnetic field $L_{\mathrm{em}}=\int d^3\mathbf{r}[\frac{1}{2}\epsilon_0\mathbf{E}(\mathbf{r},t)\cdot\mathbf{E}^*(\mathbf{r},t)-\frac{1}{2\mu_0}\mathbf{B}(\mathbf{r},t)\cdot\mathbf{B}^*(\mathbf{r},t)]$ can be written as $L_{\mathrm{em}}=\frac{l}{2}\sum_{\mathbf{q},\lambda}[\frac{\partial Q_{\mathbf{q},\lambda}(t)}{\partial t}\frac{\partial Q_{-\mathbf{q},\lambda}(t)}{\partial t}-\omega_{\mathbf{q}}^2Q_{\mathbf{q},\lambda}(t)Q_{-\mathbf{q},\lambda}(t)]$. The Hamiltonian is thus $H_{\mathrm{em}}=\sum_{\mathbf{q},\lambda}[\frac{1}{2l}P_{\mathbf{q},\lambda}(t)P_{-\mathbf{q},\lambda}(t)+\frac{l}{2}\omega_{\mathbf{q}}^2Q_{\mathbf{q},\lambda}(t)Q_{-\mathbf{q},\lambda}(t)]$, where $P_{\mathbf{q},\lambda}(t)=l\frac{\partial Q_{-\mathbf{q},\lambda}(t)}{\partial t}$ denotes the momentum conjugate to $Q_{\mathbf{q},\lambda}(t)$. The quantization of the electromagnetic field proceeds with identifying $\hat{Q}_{\mathbf{q},\lambda}(t)$ and $\hat{P}_{\mathbf{q},\lambda}(t)$ as operators which obey the commutation relation $[\hat{Q}_{\mathbf{q},\lambda}(t),\hat{P}_{\mathbf{q}',\lambda'}(t)]=i\hbar\delta_{\lambda,\lambda'}\delta_{q,q'}$. To this end, the Hamiltonian reads as

$$H_{\mathrm{em}}=\sum_{\mathbf{q},\lambda}\hbar\omega_{\mathbf{q}}\hat{\mathbf{f}}^\dagger_{\mathbf{q},\lambda}(t)\hat{\mathbf{f}}_{\mathbf{q},\lambda}(t), \tag{10}$$

where $\hat{\mathbf{f}}^\dagger_{\mathbf{q},\lambda}(t)=\sqrt{\frac{\omega_{\mathbf{q}}l}{2\hbar}}[\hat{Q}_{-\mathbf{q},\lambda}(t)-\frac{i}{\omega_{\mathbf{q}}l}\hat{P}_{\mathbf{q},\lambda}(t)]$ and $\hat{\mathbf{f}}_{\mathbf{q},\lambda}(t)=\sqrt{\frac{\omega_{\mathbf{q}}l}{2\hbar}}[\hat{Q}_{\mathbf{q},\lambda}(t)+\frac{i}{\omega_{\mathbf{q}}l}\hat{P}_{-\mathbf{q},\lambda}(t)]$ are creation and annihilation operators of photons with wave vector $\mathbf{q}$ and polarization λ, respectively.

C. Interaction of the magnetic chain with the waveguide field

The Hamiltonian

$$H_{\mathrm{int}}=-\mu\sum_n\hat{\mathbf{B}}(\mathbf{r}_n,t)\cdot\hat{\mathbf{S}}_n-\mu\sum_n\hat{\mathbf{B}}(\mathbf{r}'_n,t)\cdot\hat{\mathbf{S}}'_n \tag{11}$$

describes the Zeeman interaction of macrospins with the waveguide field. Here $\hat{\mathbf{B}}(\mathbf{r},t)$ is the total magnetic induction acting on a magnetic sphere, which is due to the quantum vacuum and the other magnetic spheres.

Powered by the vector potential (5) and the mode functions (8), we find that the magnetic inductions of $\mathrm{TE}_{m,m'}$ and $\mathrm{TM}_{m,m'}$ modes of the waveguide are

$$\begin{aligned}
\hat{\mathbf{B}}_{\mathrm{TE}_{m,m'}}(\mathbf{r},t)=&\sum_{\mathbf{q}}\sqrt{\frac{2\hbar}{\epsilon_0\omega_{\mathbf{q}}abl}}\frac{c}{\Omega_{m,m'}}e^{iqx}\\
&\times\left[-\left(\frac{\Omega_{m,m'}}{c}\right)^2\cos\left(\frac{m\pi}{a}y\right)\cos\left(\frac{m'\pi}{b}z\right)\mathbf{e}_x\right.\\
&+iq\frac{m\pi}{a}\sin\left(\frac{m\pi}{a}y\right)\cos\left(\frac{m'\pi}{b}z\right)\mathbf{e}_y\\
&\left.+iq\frac{m'\pi}{b}\cos\left(\frac{m\pi}{a}y\right)\sin\left(\frac{m'\pi}{b}z\right)\mathbf{e}_z\right]\hat{\mathbf{f}}_{\mathbf{q}}\\
&+\mathrm{H.c.},\\
\hat{\mathbf{B}}_{\mathrm{TM}_{m,m'}}(\mathbf{r},t)=&\sum_{\mathbf{q}}\sqrt{\frac{2\hbar\omega_{\mathbf{q}}}{\epsilon_0abl}}\frac{1}{\Omega_{m,m'}}\frac{|q|}{q}e^{iqx}\\
&\times\left[-\frac{im'\pi}{b}\sin\left(\frac{m\pi}{a}y\right)\cos\left(\frac{m'\pi}{b}z\right)\mathbf{e}_y\right.\\
&\left.+\frac{im\pi}{a}\cos\left(\frac{m\pi}{a}y\right)\sin\left(\frac{m'\pi}{b}z\right)\mathbf{e}_z\right]\hat{\mathbf{f}}_{\mathbf{q}}+\mathrm{H.c.}
\end{aligned} \tag{12}$$

III. PHOTON-MEDIATED INTERACTION OF TWO MAGNETIC SPHERES

In the following we consider *the dispersive regime*. We focus on the magnonic subsystem and eliminate the direct magnon-photon interaction in favor of the photon-mediated magnon-magnon interaction.

The photon-mediated interaction of *two* magnetic spheres in the *unbounded space* reduces to the magnetostatic dipole-dipole interaction, when the retardation effect is small (see Appendix A). Here we explore the photon-mediated interaction of two magnetic spheres embedded in the *waveguide*, namely, a macrospin $\hat{\mathbf{S}}$ at position $\mathbf{r} = (x, y_s, z_s)$ and a macrospin $\hat{\mathbf{S}}'$ at position $\mathbf{r}' = (x', y_s, z_s)$. The Hamiltonian

$$\begin{aligned} H &= H_m + H_{em} + H_{int} \\ &= -\mu \mathbf{B}_1 \cdot \hat{\mathbf{S}} - \mu \mathbf{B}_2 \cdot \hat{\mathbf{S}}' + \sum_{\mathbf{q},\lambda} \hbar\omega_{\mathbf{q}} \hat{\mathbf{f}}^\dagger_{\mathbf{q},\lambda} \hat{\mathbf{f}}_{\mathbf{q},\lambda} \\ &\quad - \mu \hat{\mathbf{B}}(\mathbf{r}, t) \cdot \hat{\mathbf{S}} - \mu \hat{\mathbf{B}}(\mathbf{r}', t) \cdot \hat{\mathbf{S}}' \end{aligned} \tag{13}$$

describes the dynamics of two macrospins [see Eqs. (1), (10), and (11)]. We use the Holstein-Primakoff transformation to write

$$\begin{aligned} H_m &= \hbar\mu B_1 \hat{\mathbf{a}}^\dagger \hat{\mathbf{a}} + \hbar\mu B_2 \hat{\mathbf{b}}^\dagger \hat{\mathbf{b}}, \\ H_{int} &= \sum_{\mathbf{q},\lambda} (\mathcal{C}_{1,\mathbf{q},\lambda} \hat{\mathbf{f}}_{\mathbf{q},\lambda} \hat{\mathbf{a}}^\dagger + \mathcal{C}_{2,\mathbf{q},\lambda} \hat{\mathbf{f}}_{\mathbf{q},\lambda} \hat{\mathbf{b}}^\dagger) + \text{H.c.}, \end{aligned} \tag{14}$$

where

$$\begin{aligned} \mathcal{C}^{\perp}_{1,\mathbf{q},\lambda=1} &= \hbar\mu \sqrt{\frac{S_1\hbar}{\epsilon_0 \omega_{\mathbf{q}} abl}} \frac{c}{\Omega_{m,m'}} e^{iqx} \\ &\quad \times \left[\left(\frac{\Omega_{m,m'}}{c} \right)^2 \cos\left(\frac{m\pi}{a} y_s \right) \cos\left(\frac{m'\pi}{b} z_s \right) \right. \\ &\quad \left. + q \frac{m\pi}{a} \sin\left(\frac{m\pi}{a} y_s \right) \cos\left(\frac{m'\pi}{b} z_s \right) \right], \\ \mathcal{C}^{\perp}_{1,\mathbf{q},\lambda=2} &= -\hbar\mu \sqrt{\frac{S_1\hbar\omega_{\mathbf{q}}}{\epsilon_0 abl}} \frac{1}{\Omega_{m,m'}} \frac{|q|}{q} e^{iqx} \\ &\quad \times \frac{m'\pi}{b} \sin\left(\frac{m\pi}{a} y_s \right) \cos\left(\frac{m'\pi}{b} z_s \right), \end{aligned} \tag{15}$$

when the external magnetic inductions are perpendicular to the chain axis, and

$$\begin{aligned} \mathcal{C}^{\parallel}_{1,\mathbf{q},\lambda=1} &= -\hbar\mu \sqrt{\frac{S_1\hbar}{\epsilon_0 \omega_{\mathbf{q}} abl}} \frac{c}{\Omega_{m,m'}} e^{iqx} \\ &\quad \times \left[iq \frac{m\pi}{a} \sin\left(\frac{m\pi}{a} y_s \right) \cos\left(\frac{m'\pi}{b} z_s \right) \right. \\ &\quad \left. - q \frac{m'\pi}{b} \cos\left(\frac{m\pi}{a} y_s \right) \sin\left(\frac{m'\pi}{b} z_s \right) \right], \\ \mathcal{C}^{\parallel}_{1,\mathbf{q},\lambda=2} &= \hbar\mu \sqrt{\frac{S_1\hbar\omega_{\mathbf{q}}}{\epsilon_0 abl}} \frac{1}{\Omega_{m,m'}} \frac{|q|}{q} e^{iqx} \\ &\quad \times \left[i \frac{m'\pi}{b} \sin\left(\frac{m\pi}{a} y_s \right) \cos\left(\frac{m'\pi}{b} z_s \right) \right. \\ &\quad \left. + \frac{m\pi}{a} \cos\left(\frac{m\pi}{a} y_s \right) \sin\left(\frac{m'\pi}{b} z_s \right) \right], \end{aligned} \tag{16}$$

when the external magnetic inductions are parallel to the chain axis. $\mathcal{C}_{2,\mathbf{q},\lambda}$ is obtained from $\mathcal{C}_{1,\mathbf{q},\lambda}$ by $S_1 \to S_2$ and $x \to x'$. Note that we have employed the rotating wave approximation (RWA) to neglect the quickly rotating terms like $\hat{\mathbf{f}}^\dagger_{\mathbf{q},\lambda} \hat{\mathbf{a}}^\dagger$ and $\hat{\mathbf{f}}^\dagger_{\mathbf{q},\lambda} \hat{\mathbf{b}}^\dagger$.

We use the Schrieffer-Wolff canonical transformation $H' = e^{\Lambda} H e^{-\Lambda}$, where $\Lambda = \sum_{\mathbf{k},\lambda} (\mathcal{I}_{\mathbf{k},\lambda} \hat{\mathbf{f}}_{\mathbf{k},\lambda} \hat{\mathbf{a}}^\dagger + \mathcal{J}_{\mathbf{k},\lambda} \hat{\mathbf{f}}_{\mathbf{k},\lambda} \hat{\mathbf{b}}^\dagger - \mathcal{I}^*_{\mathbf{k},\lambda} \hat{\mathbf{f}}^\dagger_{\mathbf{k},\lambda} \hat{\mathbf{a}} - \mathcal{J}^*_{\mathbf{k},\lambda} \hat{\mathbf{f}}^\dagger_{\mathbf{k},\lambda} \hat{\mathbf{b}})$, $\mathcal{I}_{\mathbf{k},\lambda} = \frac{\mathcal{C}_{1,\mathbf{k},\lambda}}{\hbar\mu B_1 - \hbar\omega_k}$, and $\mathcal{J}_{\mathbf{k},\lambda} = \frac{\mathcal{C}_{2,\mathbf{k},\lambda}}{\hbar\mu B_2 - \hbar\omega_k}$. Up to second order of $\mathcal{C}_{1,2\mathbf{k},\lambda}$ indeed $H' \approx H'_m + H'_{em}$, where H'_{em} can be written only in terms of photon creation and annihilation operators, and the effective magnetic Hamiltonian reads as

$$\begin{aligned} H'_m &= \hbar(\mu B_1 + \omega_{1,L}) \hat{\mathbf{a}}^\dagger \hat{\mathbf{a}} + \hbar(\mu B_2 + \omega_{2,L}) \hat{\mathbf{b}}^\dagger \hat{\mathbf{b}} \\ &\quad + \tfrac{1}{2}[J(B_1, |x' - x|, y_s, z_s) + J(B_2, |x' - x|, y_s, z_s)] \hat{\mathbf{a}} \hat{\mathbf{b}}^\dagger \\ &\quad + \text{H.c.}, \end{aligned} \tag{17}$$

where $\hbar\omega_{1,2L} = \sum_{\mathbf{k},\lambda} \frac{|\mathcal{C}_{1,2\mathbf{k},\lambda}|^2}{\hbar\mu B_{1,2} - \hbar\omega_{\mathbf{k}}} \propto S_{1,2}$ [see Eqs. (15) and (16)] is the Lamb shift of the Larmor frequency $\mu B_{1,2}$ of the macrospin $S_{1,2}$, and

$$J(B_1, |x' - x|, y_s, z_s) \equiv \sum_{\mathbf{k},\lambda} \frac{\mathcal{C}^*_{1,\mathbf{k},\lambda}(x, y_s, z_s) \mathcal{C}_{2,\mathbf{k},\lambda}(x', y_s, z_s)}{\hbar\mu B_1 - \hbar\omega_{\mathbf{k}}}. \tag{18}$$

Here,

$$\zeta_{1,2} = \hbar\mu B_{1,2} + \hbar\omega_{1,2L} \tag{19}$$

are "onsite energies" which can be equal if $B_1 = B_2$ and $S_1 = S_2$. The last term of Eq. (17) describes photon-mediated interaction of two magnetic spheres.

A few remarks concerning the photon-mediated interaction of two macrospins are in order. (i) In the dispersive regime, the magnon and the waveguide modes are detuned from each other, i.e., $|\hbar\mu B_{1,2} - \hbar\omega_{\mathbf{k}}| > |\mathcal{C}_{1,2,k}|$. (ii) The macrospin $S_{1,2}$ precesses about the static magnetic induction $\mathbf{B}_{1,2}$ with the Larmor frequency $\mu B_{1,2}$. The interaction between two macrospins is retarded by $\frac{1}{c}|\mathbf{r}' - \mathbf{r}|$ which is small when $\frac{\mu B_{1,2}}{c}|\mathbf{r}' - \mathbf{r}| \ll 1$. (iii) The metallic walls impose severe boundary conditions on the electromagnetic field inside the waveguide. It follows that the photon-mediated interactions of two macrospins in *unbounded* and *bounded* spaces are distinct, even when the retardation effect is small (see Appendixes B and C). (iv) We have assumed that the Zeeman interaction of a macrospin with the static magnetic induction $\hbar\mu B_{1,2}$ is much greater than its photon-mediated interaction with the neighboring macrospins $w_{1,2}$. In other words, only the external magnetic induction, whether perpendicular or parallel to the chain axis, determines the ground state of the system. For example, when $S_{1,2} = 10^{16}$, $B_{1,2} = 0.1$ T, $d_{1,2} = 0.5$ mm, $a = b = 10$ mm, $y_s = \frac{a}{4}$, and $z_s = 0$, then $|w_{1,2}| \sim 10^{-4}\hbar\mu B_{1,2}$. (v) It is noteworthy that *weak* magnetic inductions are not able to dictate the ground state. In this regime, the chain of magnetic spheres exhibits shape anisotropy [60]. This anisotropy manifests to some extent in the collective spin wave modes of the system [61,62]. (vi) We have assumed that each magnetic sphere acts as a macrospin. This is reasonable when magnetic spheres are not too close to each other: each

magnetic sphere generates an almost uniform magnetic induction inside its neighbors.

IV. A CHAIN OF MAGNETIC SPHERES INSIDE A WAVEGUIDE

Now we write the Hamiltonian

$$H'_m = \sum_{n=1}^{N}(\zeta_1 \hat{\mathbf{a}}_n^\dagger \hat{\mathbf{a}}_n + \zeta_2 \hat{\mathbf{b}}_n^\dagger \hat{\mathbf{b}}_n) + \sum_{n=1}^{N}(w_1 \hat{\mathbf{a}}_n \hat{\mathbf{b}}_n^\dagger + \text{H.c.}) + \sum_{n=1}^{N-1}(w_2 \hat{\mathbf{a}}_{n+1} \hat{\mathbf{b}}_n^\dagger + \text{H.c.}) \tag{20}$$

to describe the low-energy collective excitations of a bipartite chain of magnetic spheres with N unit cells embedded in a waveguide. Note that the Lamb shift of the outermost left and right macrospins of the chain may be different from that of the bulk macrospins. We have assumed that the additional magnetic inductions δB_L and δB_R are applied to ensure that the onsite energies of equivalent sites of the bipartite chain are equal. This allows topologically protected edge states to bloom [59]. Moreover, the Hamiltonian includes the photon-mediated interaction of magnetic spheres. Here

$$w_1 = \frac{J(B_1, d_1, y_s, z_s) + J(B_2, d_1, y_s, z_s)}{2},$$
$$w_2 = \frac{J(B_1, d_2, y_s, z_s) + J(B_2, d_2, y_s, z_s)}{2} \tag{21}$$

describe intracoupling of macrospins at a distance d_1, and intercoupling of macrospins at a distance d_2, respectively.

We first concentrate on an *infinite* chain of magnetic spheres inside a waveguide. Indeed the properties of an infinite system are independent of its ends, thus we adopt periodic boundary conditions to rewrite the Hamiltonian (20) in the momentum space. The Hamiltonian in the basis $\Phi_k^\dagger = (\hat{\mathbf{a}}_k^\dagger, \hat{\mathbf{b}}_k^\dagger)$ is $H'_m = \sum_k \Phi_k^\dagger \mathcal{H}'_m(k) \Phi_k$, where

$$\mathcal{H}'_m(k) = \begin{bmatrix} \zeta_1 & \eta_k \\ \eta_k^* & \zeta_2 \end{bmatrix}, \tag{22}$$

k is the lattice momentum, and $\eta_k = w_1 + w_2 e^{-ikd}$. The Hamiltonian has an inversion symmetry when $\zeta_1 = \zeta_2$: explicitly, $\mathcal{I}\mathcal{H}'_m(k)\mathcal{I}^{-1} = \mathcal{H}'_m(-k)$ where $\mathcal{I} = \tau_x$ (τ_i are Pauli matrices and τ_0 is the identity matrix).

The Hamiltonian H'_m can be diagonalized by a Bogoliubov transformation, given by

$$\hat{\mathbf{c}}_{1k} = o_{1k}\hat{\mathbf{a}}_k + p_{1k}\hat{\mathbf{b}}_k,$$
$$\hat{\mathbf{c}}_{2k} = o_{2k}\hat{\mathbf{a}}_k + p_{2k}\hat{\mathbf{b}}_k. \tag{23}$$

Rewritten in terms of the introduced quasiparticles the Hamiltonian takes the form

$$H'_m = \sum_k (E_{1k}\hat{\mathbf{c}}_{1k}^\dagger \hat{\mathbf{c}}_{1k} + E_{2k}\hat{\mathbf{c}}_{2k}^\dagger \hat{\mathbf{c}}_{2k}). \tag{24}$$

The commutation relations $[\hat{\mathbf{c}}_{1k}, \hat{\mathbf{c}}_{1k}^\dagger] = [\hat{\mathbf{c}}_{2k}, \hat{\mathbf{c}}_{2k}^\dagger] = 1$ and the Heisenberg equations of motion $[\hat{\mathbf{c}}_{1k}, H'_m] = E_{1k}\hat{\mathbf{c}}_{1k}$ and $[\hat{\mathbf{c}}_{2k}, H'_m] = E_{2k}\hat{\mathbf{c}}_{2k}$ lead to the following eigenproblem:

$$\begin{bmatrix} \zeta_1 & \eta_k^* \\ \eta_k & \zeta_2 \end{bmatrix} \begin{bmatrix} o_{1,2k} \\ p_{1,2k} \end{bmatrix} = E_{1,2k} \begin{bmatrix} o_{1,2k} \\ p_{1,2k} \end{bmatrix} \tag{25}$$

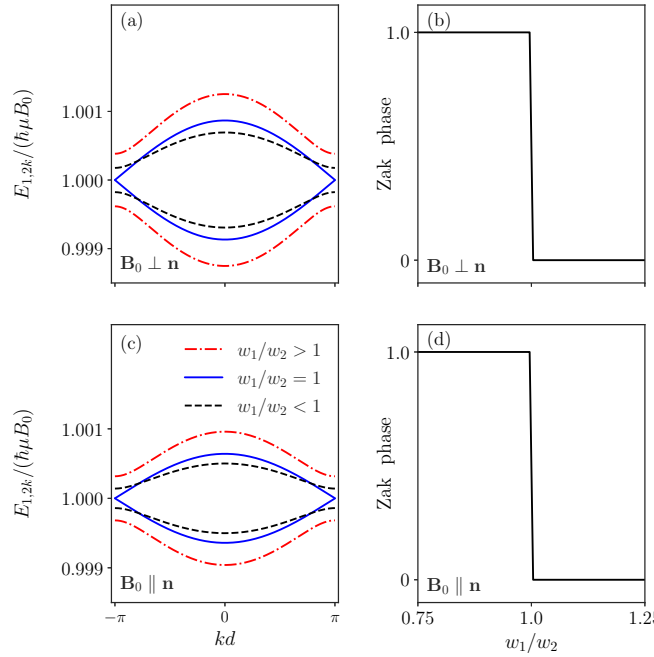

FIG. 2. (a) The energy spectrum of the Bogoliubov quasiparticle excitations of the chain $E_{1,2k}$ versus kd for $d_1 \in \{0.4, 0.5, 0.6\}$ mm. (b) The Zak phase φ_{Zak} versus w_1/w_2. Here $\mathbf{B}_0 \perp \mathbf{n}$. Similar plots for the case of $\mathbf{B}_0 \parallel \mathbf{n}$ are in (c) and (d). In all plots $S_1 = S_2 = 10^{16}$, $B_0 = 0.1$ T, $d_2 = 0.5$ mm, $a = b = 10$ mm, $y_s = \frac{a}{4}$, and $z_s = 0$.

whose solution straightforwardly provides the coefficients $o_{1,2k}$ and $p_{1,2k}$, and the energies

$$E_{1,2k} = \frac{1}{2}(\zeta_1 + \zeta_2) \pm \frac{1}{2}\sqrt{(\zeta_1 - \zeta_2)^2 + 4|\eta_k|^2}. \tag{26}$$

The spectrum has an overall nonzero gap. However, the gap can be closed at $kd = \pm\pi$ if first $B_1 = B_2$ and $S_1 = S_2$ to ensure that onsite energies are equal, and second $w_1 = w_2$. Hereafter, we assume that $\mathbf{B}_1 = \mathbf{B}_2 \equiv \mathbf{B}_0$.

There is a strong similarity between the chain of magnetic spheres inside a waveguide and the SSH system. The two limiting cases of $w_1 \neq 0$, $w_2 = 0$ and $w_1 = 0$, $w_2 \neq 0$, with dominant intracoupling and intercoupling, respectively, correspond to distinct dimerized regimes of the SSH system. A topological transition somewhere in-between these two limits is thus expected. We find that two topologically distinct phases of the chain emerge for $w_1/w_2 > 1$ and $w_1/w_2 < 1$, and the transition is characterized by closing and reopening the gap at $w_1/w_2 = 1$. To confirm this, we calculate the Zak phase [63]

$$\varphi_{\text{Zak}} = -i \int_{1^{\text{st}}\ \text{BZ}} \langle \Psi_{1,2k} | \partial_k | \Psi_{1,2k} \rangle dk, \tag{27}$$

where $|\Psi_{1,2k}\rangle = [o_{1,2k}, p_{1,2k}]^T$ and the integral is taken over the first Brillouin zone. The Zak phase has been used in study of various magnonic crystals (see, e.g., Ref. [64] and references therein).

As a concrete example, we take $S_1 = S_2 = 10^{16}$, $B_0 = 0.1$ T, $d_2 = 0.5$ mm, $a = b = 10$ mm, $y_s = \frac{a}{4}$, and $z_s = 0$. Figure 2(a) depicts the bulk excitation spectrum of the chain $E_{1,2k}$ as a function of kd when $\mathbf{B}_0 \perp \mathbf{n}$. The closing and reopening the gap occurs at $w_1/w_2 = 1$. Figure 2(b) shows the

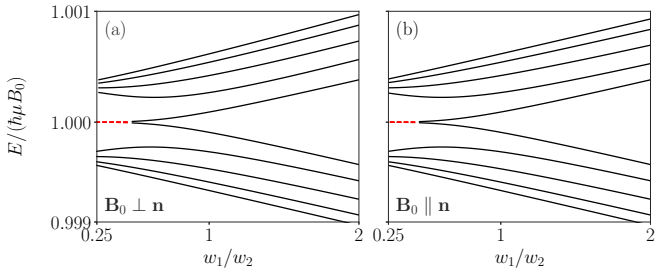

FIG. 3. The energies of a finite chain with $N = 5$ unit cells versus w_1/w_2. The energies of bulk states (in black solid) and localized end modes (in dashed) for the case of (a) $\mathbf{B}_0 \perp \mathbf{n}$ and (b) $\mathbf{B}_0 \parallel \mathbf{n}$. All the other parameters are the same as in Fig. 2.

Zak phase as a function of w_1/w_2. The Zak phase is quantized, revealing two topologically distinct phases for $w_1/w_2 < 1$ and $w_1/w_2 > 1$. Figures 2(c) and 2(d) pertaining to the case of $\mathbf{B}_0 \parallel \mathbf{n}$ convey the same message.

Up to now, we have studied topologically distinct phases of an infinite chain of magnetic spheres inside the waveguide. However, the physical consequence of different Zak phases, i.e., the bulk invariant, becomes more apparent for a finite chain. Here we consider a *finite* chain of N unit cells, and examine the link between the quantized Zak phase and the presence of topologically protected end states. We remind that it has been recently recognized that even *Hermitian* topological materials can exhibit breakdown of the bulk-edge correspondence [65–67]. We numerically diagonalize the quadratic bosonic Hamiltonian (20). As a concrete example, we take $N = 5$. Figure 3 demonstrates that all states are singly degenerate delocalized states when $w_1/w_2 > 0.45$. Remarkably, a pair of doubly degenerate localized modes which are topological edge states appear within the gap when $w_1/w_2 < 0.45$, which reveals a connection between the bulk invariant and the boundary invariant, i.e., the number of edge states. For the case of $N = 40$, the wave functions of the localized edge states are depicted in Fig. 4. This confirms the bulk-boundary correspondence: For $w_1/w_2 < 1$, the system is in a topological phase characterized by $\varphi_{\text{Zak}} = \pi$ and is expected to host topologically protected localized edge states. Now it is legitimate to assert that for $w_1/w_2 > 1$ the finite chain is in a *topologically trivial* phase, while for $w_1/w_2 < 1$ the finite chain is in a topological phase.

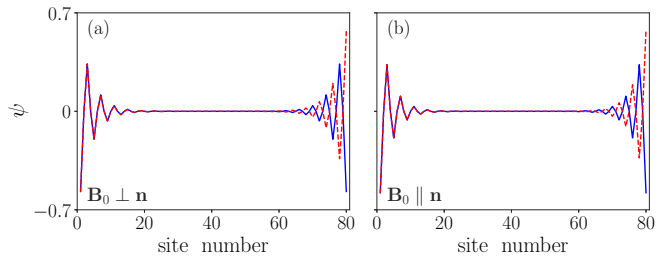

FIG. 4. Wave functions ψ_L (in red) and ψ_R (in blue) with energy $\hbar\mu B_0$, for the case of (a) $\mathbf{B}_0 \perp \mathbf{n}$ and (b) $\mathbf{B}_0 \parallel \mathbf{n}$. Here $N = 40$ and $d_1 = 0.6$ mm. All the other parameters are the same as in Fig. 2.

V. CONCLUSION

In conclusion, we have studied a one-dimensional bipartite chain of magnetic spheres inside a rectangular metallic waveguide. The magnetic spheres are subjected to external static magnetic inductions which are either perpendicular or parallel to the chain axis. In the dispersive regime, the waveguide photon-mediated interaction, which is quite different from that in the free space, between magnetic spheres turn the chain into a magnonic crystal. The magnonic crystal exhibits two topologically distinct gapped phases, and the transition is characterized by closing and reopening the gap. Topological end states form at the boundaries of the magnonic crystal in accordance with the bulk-boundary correspondence. Magnetically *tunable* topological magnon modes may secure their place in future applications.

Generally speaking, the interactions of electric and magnetic dipoles are quite similar. Indeed, bipartite chains of metallic nanoparticles [48] and magnetic microspheres [59] embedded in the free space share some common topological features. A recent study of a chain of plasmonic nanoparticles inside a metallic waveguide has concluded that the strong light-matter coupling leads to breakdown of the bulk-edge correspondence. The Hamiltonian of the chain of plasmonic nanoparticles consists of three terms, namely, the dipolar Hamiltonian H_{dp} which includes the dipole-dipole interactions, the photonic Hamiltonian H_{ph}, and the light-matter coupling Hamiltonian $H_{\text{dp-ph}}$ [68]. It deserves a further study of whether this approach overweights the first term of the Hamiltonian since the photon-mediated electric dipole-dipole interaction is already a consequence of the interaction of the electric dipoles with the photonic field.

APPENDIX A: INTERACTION OF TWO MAGNETIC SPHERES IN THE UNBOUNDED SPACE

Here we focus on the photon-mediated interaction of *two* magnetic spheres in the *unbounded space*, namely, a macrospin $\hat{\mathbf{S}}$ at position $\mathbf{r}$ and a macrospin $\hat{\mathbf{S}}'$ at position $\mathbf{r}'$. The Hamiltonian H describes the dynamics of the system [see Eq. (13)].

We choose three mutually perpendicular unit vectors $\mathbf{n}_1$, $\mathbf{n}_2$, and $\mathbf{n}_3 \parallel \mathbf{B}_{1,2}$, and express the spin operators in terms of the bosonic operator as

$$\begin{aligned}
\hat{\mathbf{S}} \cdot \mathbf{n}_1 &= \frac{S_+ + S_-}{2} = \frac{\hbar}{2}\sqrt{2S_1}(\hat{\mathbf{a}} + \hat{\mathbf{a}}^\dagger), \\
\hat{\mathbf{S}} \cdot \mathbf{n}_2 &= \frac{S_+ - S_-}{2i} = \frac{\hbar}{2i}\sqrt{2S_1}(\hat{\mathbf{a}} - \hat{\mathbf{a}}^\dagger), \\
\hat{\mathbf{S}} \cdot \mathbf{n}_3 &= \hbar(S_1 - \hat{\mathbf{a}}^\dagger\hat{\mathbf{a}}).
\end{aligned} \tag{A1}$$

We write the magnetic induction in a cubic region of space of volume $V \to \infty$ as

$$\hat{\mathbf{B}}(\mathbf{r}, t) = \sum_{\mathbf{k},\lambda} i\sqrt{\frac{\mu_0\hbar\omega_{\mathbf{k}}}{2V}}\mathbf{e}_{\mathbf{k}\lambda}(\hat{\mathbf{f}}_{\mathbf{k},\lambda}e^{i\mathbf{k}\cdot\mathbf{r}} - \hat{\mathbf{f}}^\dagger_{\mathbf{k},\lambda}e^{-i\mathbf{k}\cdot\mathbf{r}}). \tag{A2}$$

Here $\omega_{\mathbf{k}} = ck$ and $\mathbf{e}_{\mathbf{k}\lambda} = \hat{\mathbf{k}} \times \mathbf{e}_\lambda$, in which three mutually perpendicular unit vectors $\mathbf{e}_1$, $\mathbf{e}_2$, and $\hat{\mathbf{k}}$ specify the polarization and direction of propagation of the mode ($\mathbf{k}$, $\lambda = 1, 2$). We

use the identity

$$\mathbf{v}\cdot\mathbf{u}=(\mathbf{v}\cdot\mathbf{n}_1)(\mathbf{u}\cdot\mathbf{n}_1)+(\mathbf{v}\cdot\mathbf{n}_2)(\mathbf{u}\cdot\mathbf{n}_2)+(\mathbf{v}\cdot\mathbf{n}_3)(\mathbf{u}\cdot\mathbf{n}_3) \tag{A3}$$

to rewrite $H_{\rm m}$ and $H_{\rm int}$ [see Eq. (14)]. Here

$$\mathcal{C}_{1\mathbf{k},\lambda}=-i\hbar\mu\sqrt{\frac{S_1\mu_0\hbar\omega_{\mathbf{k}}}{2V}}\mathbf{e}_{\mathbf{k}\lambda}\cdot\frac{(\mathbf{n}_1+i\mathbf{n}_2)}{\sqrt{2}}e^{i\mathbf{k}.\mathbf{r}},$$

$$\mathcal{C}_{2\mathbf{k},\lambda}=-i\hbar\mu\sqrt{\frac{S_2\mu_0\hbar\omega_{\mathbf{k}}}{2V}}\mathbf{e}_{\mathbf{k}\lambda}\cdot\frac{(\mathbf{n}_1+i\mathbf{n}_2)}{\sqrt{2}}e^{i\mathbf{k}.\mathbf{r}'}. \tag{A4}$$

We use the Schrieffer-Wolff canonical transformation to write $H'\approx H'_{\rm m}+H'_{\rm em}$ [see Eq. (17)]. The task is now to calculate $J(B_1,|\mathbf{r}'-\mathbf{r}|)\equiv\sum_{\mathbf{k},\lambda}\frac{\mathcal{C}^*_{1,\mathbf{k},\lambda}\mathcal{C}_{2,\mathbf{k},\lambda}}{\hbar\mu B_1-\hbar\omega_{\mathbf{k}}}$. We choose three mutually perpendicular unit vectors $\mathbf{u}_1$, $\mathbf{u}_2$, and $\mathbf{u}_3=(\mathbf{r}'-\mathbf{r})/|\mathbf{r}'-\mathbf{r}|$. We represent $\mathbf{k}=k\sin\theta\cos\varphi\mathbf{u}_1+k\sin\theta\sin\varphi\mathbf{u}_2+k\cos\theta\mathbf{u}_3$ in this coordinate system and convert the summation over $\mathbf{k}$ to an integration, that is, $\sum_{\mathbf{k}}=\frac{V}{(2\pi)^3}\int d^3\mathbf{k}=\frac{V}{(2\pi c)^3}\int\omega_{\mathbf{k}}^2d\omega_{\mathbf{k}}\int_0^{2\pi}d\varphi\int_0^{\pi}\sin\theta\,d\theta$. It follows that

$$\begin{aligned}
&J(B_1,|\mathbf{r}'-\mathbf{r}|)\\
&=-\sum_{\mathbf{k},\lambda}\frac{\hbar^2\mu^2\mu_0\omega_{\mathbf{k}}\sqrt{S_1S_2}}{4V(\mu B_1-\omega_{\mathbf{k}})}[(\mathbf{e}_{\mathbf{k}\lambda}.\mathbf{n}_1)^2+(\mathbf{e}_{\mathbf{k}\lambda}.\mathbf{n}_2)^2]e^{i\mathbf{k}\cdot(\mathbf{r}'-\mathbf{r})}\\
&=-\sum_{\mathbf{k}}\frac{\hbar^2\mu^2\mu_0\omega_{\mathbf{k}}\sqrt{S_1S_2}}{4V(\mu B_1-\omega_{\mathbf{k}})}[1+(\mathbf{n}_3\cdot\hat{\mathbf{k}})^2]e^{i\mathbf{k}\cdot(\mathbf{r}'-\mathbf{r})}\\
&=-\frac{\hbar^2\mu^2\mu_0\sqrt{S_1S_2}}{32\pi^3c^3}\int\frac{\omega_{\mathbf{k}}^3}{\mu B_1-\omega_{\mathbf{k}}}\mathrm{d}\omega_{\mathbf{k}}\int_0^{\pi}e^{i\mathbf{k}\cdot(\mathbf{r}'-\mathbf{r})}\sin\theta\,d\theta\\
&\quad\times\int_0^{2\pi}[1+(\mathbf{n}_3\cdot\hat{\mathbf{k}})^2]d\varphi.
\end{aligned}\tag{A5}$$

We note that

$$\begin{aligned}
&\int_0^{2\pi}(\mathbf{n}_3\cdot\hat{\mathbf{k}})^2d\varphi\\
&=\pi[(\mathbf{n}_3\cdot\mathbf{u}_1)^2+(\mathbf{n}_3\cdot\mathbf{u}_2)^2]\sin^2\theta+2\pi(\mathbf{n}_3\cdot\mathbf{u}_3)^2\cos^2\theta\\
&=\pi[1-(\mathbf{n}_3\cdot\mathbf{u}_3)^2]\sin^2\theta+2\pi(\mathbf{n}_3\cdot\mathbf{u}_3)^2\cos^2\theta.
\end{aligned}\tag{A6}$$

Moreover,

$$\begin{aligned}
f_1(kr)&\equiv\int_0^{\pi}\sin\theta e^{ikr\cos\theta}d\theta=\frac{2\sin kr}{kr},\\
f_2(kr)&\equiv\int_0^{\pi}\sin\theta\cos^2\theta e^{ikr\cos\theta}d\theta\\
&=\frac{2\sin kr}{kr}+\frac{4\cos kr}{(kr)^2}-\frac{4\sin kr}{(kr)^3}.
\end{aligned}\tag{A7}$$

Thus,

$$\begin{aligned}
J(B_1,|\mathbf{r}'-\mathbf{r}|)&=-\frac{\hbar^2\mu^2\mu_0\sqrt{S_1S_2}}{32\pi^2c^3}\int\frac{\omega_{\mathbf{k}}^3}{\mu B_1-\omega_{\mathbf{k}}}d\omega_{\mathbf{k}}\int_0^{\pi}e^{ik|\mathbf{r}'-\mathbf{r}|\cos\theta}\sin\theta[[3-(\mathbf{n}_3\cdot\mathbf{u}_3)^2]-[1-3(\mathbf{n}_3\cdot\mathbf{u}_3)^2]\cos^2\theta]d\theta\\
&=-\frac{\hbar^2\mu^2\mu_0\sqrt{S_1S_2}}{32\pi^2c^3}\int\frac{\omega_{\mathbf{k}}^3}{\mu B_1-\omega_{\mathbf{k}}}[[3-(\mathbf{n}_3\cdot\mathbf{u}_3)^2]f_1(k|\mathbf{r}'-\mathbf{r}|)-[1-3(\mathbf{n}_3\cdot\mathbf{u}_3)^2]f_2(k|\mathbf{r}'-\mathbf{r}|)]d\omega_{\mathbf{k}}\\
&=-\frac{\hbar^2\mu^2\mu_0\sqrt{S_1S_2}}{32\pi^2|\mathbf{r}'-\mathbf{r}|^3}\int\frac{x^3}{\frac{\mu B_1}{c}|\mathbf{r}'-\mathbf{r}|-x}[[3-(\mathbf{n}_3\cdot\mathbf{u}_3)^2]f_1(x)-[1-3(\mathbf{n}_3\cdot\mathbf{u}_3)^2]f_2(x)]dx\\
&=-\frac{\hbar^2\mu^2\mu_0\sqrt{S_1S_2}}{16\pi|\mathbf{r}'-\mathbf{r}|^3}f_{\rm dd}\left(\frac{\mu B_1}{c}|\mathbf{r}'-\mathbf{r}|\right),
\end{aligned}\tag{A8}$$

where

$$f_{\rm dd}(x)=[3-(\mathbf{n}_3\cdot\mathbf{u}_3)^2]x^2\cos x-[1-3(\mathbf{n}_3\cdot\mathbf{u}_3)^2](x^2\cos x+2x\sin x-2\cos x). \tag{A9}$$

We remind that $\mathbf{n}_3$ is a unit vector in the dierection of major components of macrospins S_1 and S_2, and $\mathbf{u}_3$ is a unit vector in the direction from S_1 to S_2. $\mu B_{1,2}$ is the Larmor precession frequency. The retardation effect is small when $\frac{\mu B_{1,2}}{c}|\mathbf{r}'-\mathbf{r}|\ll 1$. In this limit,

$$J(B_{1,2},|\mathbf{r}'-\mathbf{r}|)\to-\frac{\hbar^2\mu^2\mu_0\sqrt{S_1S_2}}{8\pi|\mathbf{r}'-\mathbf{r}|^3}[1-3(\mathbf{n}_3\cdot\mathbf{u}_3)^2] \tag{A10}$$

represents the celebrated magnetostatic dipole-dipole interaction in the unbounded space.

APPENDIX B: EXPLICIT FORM OF $J(B_1,|x'-x|,y_{\rm s},z_{\rm s})$

Here we present the explicit form of $J(B_1,|x'-x|,y_{\rm s},z_{\rm s})$ for two magnetic spheres embedded in the waveguide:

$$\begin{aligned}
J^{\perp}(B_1,|x'-x|,y_{\rm s},z_{\rm s})=\frac{\hbar^2\mu^2\sqrt{S_1S_2}}{2\pi\epsilon_0ab}\sum_{m,m'}\Bigg\{&\left(\frac{\Omega_{m,m'}}{c}\right)^2\cos^2\left(\frac{m\pi}{a}y_{\rm s}\right)\cos^2\left(\frac{m'\pi}{b}z_{\rm s}\right)\int_{-\infty}^{\infty}\frac{e^{ik_x(x-x')}}{\omega_{\mathbf{k}}(\mu B_1-\omega_{\mathbf{k}})}dk_x\\
&+\left(\frac{c}{\Omega_{m,m'}}\right)^2\left(\frac{m\pi}{a}\right)^2\sin^2\left(\frac{m\pi}{a}y_{\rm s}\right)\cos^2\left(\frac{m'\pi}{b}z_{\rm s}\right)\int_{-\infty}^{\infty}\frac{k_x^2e^{ik_x(x-x')}}{\omega_{\mathbf{k}}(\mu B_1-\omega_{\mathbf{k}})}dk_x
\end{aligned}$$

$$- 2\frac{m\pi}{a}\sin\left(\frac{m\pi}{a}y_s\right)\cos\left(\frac{m\pi}{a}y_s\right)\cos^2\left(\frac{m'\pi}{b}z_s\right)\int_{-\infty}^{\infty}\frac{k_x e^{ik_x(x-x')}}{\omega_{\mathbf{k}}(\mu B_1-\omega_{\mathbf{k}})}dk_x$$
$$+\frac{1}{\Omega_{m,m'}^2}\left(\frac{m'\pi}{b}\right)^2\sin^2\left(\frac{m\pi}{a}y_s\right)\cos^2\left(\frac{m'\pi}{b}z_s\right)\int_{-\infty}^{\infty}\frac{\omega_{\mathbf{k}}e^{ik_x(x-x')}}{\mu B_1-\omega_{\mathbf{k}}}dk_x\Bigg\}, \tag{B1}$$

when the external magnetic inductions are perpendicular to the chain axis, and

$$J^{\parallel}(B_1,|x'-x|,y_s,z_s)=\frac{\hbar^2\mu^2\sqrt{S_1S_2}}{2\pi\epsilon_0 ab}\sum_{m,m'}\Bigg\{\left(\frac{c}{\Omega_{m,m'}}\right)^2\left(\frac{m\pi}{a}\right)^2\sin^2\left(\frac{m\pi}{a}y_s\right)\cos^2\left(\frac{m'\pi}{b}z_s\right)\int_{-\infty}^{\infty}\frac{k_x^2e^{ik_x(x-x')}}{\omega_{\mathbf{k}}(\mu B_1-\omega_{\mathbf{k}})}dk_x$$
$$+\left(\frac{c}{\Omega_{m,m'}}\right)^2\left(\frac{m'\pi}{b}\right)^2\cos^2\left(\frac{m\pi}{a}y_s\right)\sin^2\left(\frac{m'\pi}{b}z_s\right)\int_{-\infty}^{\infty}\frac{k_x^2e^{ik_x(x-x')}}{\omega_{\mathbf{k}}(\mu B_1-\omega_{\mathbf{k}})}dk_x$$
$$+\frac{1}{\Omega_{m,m'}^2}\left(\frac{m\pi}{a}\right)^2\cos^2\left(\frac{m\pi}{a}y_s\right)\sin^2\left(\frac{m'\pi}{b}z_s\right)\int_{-\infty}^{\infty}\frac{\omega_{\mathbf{k}}e^{ik_x(x-x')}}{\mu B_1-\omega_{\mathbf{k}}}dk_x$$
$$+\frac{1}{\Omega_{m,m'}^2}\left(\frac{m'\pi}{b}\right)^2\sin^2\left(\frac{m\pi}{a}y_s\right)\cos^2\left(\frac{m'\pi}{b}z_s\right)\int_{-\infty}^{\infty}\frac{\omega_{\mathbf{k}}e^{ik_x(x-x')}}{\mu B_1-\omega_{\mathbf{k}}}dk_x\Bigg\}, \tag{B2}$$

when the external magnetic inductions are parallel to the chain axis. The evaluation of the above integrals is presented in the next Appendix.

APPENDIX C: EVALUATION OF INTEGRALS

Let us assume that $\alpha>0$ and $1>\beta\geqslant 0$. The following integrals are of particular use:

$$E_1(\alpha)\equiv\int_{-\infty}^{\infty}\frac{e^{ik\alpha}}{\sqrt{k^2+1}}dk=2K_0(|\alpha|),$$
$$E_2(\alpha,\beta)\equiv\int_{-\infty}^{\infty}\frac{e^{ik\alpha}}{\sqrt{k^2+1}-\beta}dk=2K_0(|\alpha|)+L(\alpha,\beta). \tag{C1}$$

Here K_0 denotes the modified Bessel function of order zero, and

$$L(\alpha,\beta)=\frac{2\pi\beta}{\sqrt{1-\beta^2}}e^{-|\alpha|\sqrt{1-\beta^2}}-2\beta^2\int_0^{\infty}\frac{e^{-|\alpha|\cosh t}}{\sinh^2 t+\beta^2}dt \tag{C2}$$

contains an integral which can be easily numerically evaluated. Now it is straightforward to compute

$$O_1(\alpha)\equiv\int_{-\infty}^{\infty}\frac{ke^{ik\alpha}}{\sqrt{k^2+1}}dk=\frac{1}{i}\frac{\partial E_1(\alpha)}{\partial\alpha},$$
$$O_2(\alpha,\beta)\equiv\int_{-\infty}^{\infty}\frac{ke^{ik\alpha}}{\sqrt{k^2+1}-\beta}dk=\frac{1}{i}\frac{\partial E_2(\alpha,\beta)}{\partial\alpha},$$
$$E_3(\alpha)\equiv\int_{-\infty}^{\infty}\frac{k^2e^{ik\alpha}}{\sqrt{k^2+1}}dk=-\frac{\partial^2E_1(\alpha)}{\partial^2\alpha},$$
$$E_4(\alpha,\beta)\equiv\int_{-\infty}^{\infty}\frac{k^2e^{ik\alpha}}{\sqrt{k^2+1}-\beta}dk=-\frac{\partial^2E_2(\alpha,\beta)}{\partial^2\alpha}. \tag{C3}$$

The case of $\alpha<0$ introduces no complications: By their definition, $E_{1,2,3,4}$ and $O_{1,2}$ are even and odd functions of α, respectively.

In the following we prove Eq. (C1) using the residue theorem from the theory of functions of a complex variable. We consider the function $f(z)=\frac{e^{iz\alpha}}{\sqrt{z^2+1}-\beta}$. The contour $\Gamma=\Gamma_1\cup\Gamma_2\cup\cdots\cup\Gamma_6$ and the adopted branch cut configuration for the multivalued function $\sqrt{z^2+1}$ are shown in Fig. 5. According to the residue theorem

$$\int_{\Gamma}f(z)dz=\frac{2\pi\beta}{\sqrt{1-\beta^2}}e^{-|\alpha|\sqrt{1-\beta^2}}. \tag{C4}$$

In the limit $R\to\infty$ and $\epsilon\to 0$ indeed

$$\int_{\Gamma_1}f(z)dz=E_2(\alpha,\beta),$$
$$\int_{\Gamma_2,\Gamma_4,\Gamma_6}f(z)dz=0. \tag{C5}$$

For Γ_3, $z=is$ and $\sqrt{(z-i)(z+i)}=i\sqrt{s^2-1}$, whereas for Γ_5, $z=is$ and $\sqrt{(z-i)(z+i)}=-i\sqrt{s^2-1}$, resulting in

$$\int_{\Gamma_3}f(z)dz=\int_{\infty}^{1}\frac{e^{-s|\alpha|}}{i\sqrt{s^2-1}-\beta}i\,ds,$$
$$\int_{\Gamma_5}f(z)dz=\int_{1}^{\infty}\frac{e^{-s|\alpha|}}{-i\sqrt{s^2-1}-\beta}i\,ds. \tag{C6}$$

Now we substitute $s=\cosh t$ and use the integral representation $K_0(|\alpha|)=\int_0^{\infty}e^{-|\alpha|\cosh t}dt$ to write

$$\int_{\Gamma_3}f(z)dz=-K_0(|\alpha|)+i\int_0^{\infty}\frac{\beta e^{-|\alpha|\cosh t}}{\sinh t+i\beta}dt,$$
$$\int_{\Gamma_5}f(z)dz=-K_0(|\alpha|)-i\int_0^{\infty}\frac{\beta e^{-|\alpha|\cosh t}}{\sinh t-i\beta}dt. \tag{C7}$$

To this end, Eqs. (C4)–(C7) confirm Eq. (C1).

Indeed, the integrals appearing in Eqs. (B1) and (B2) can be expressed in terms of the above $E_{1,2,3,4}$ and $O_{1,2}$ functions.

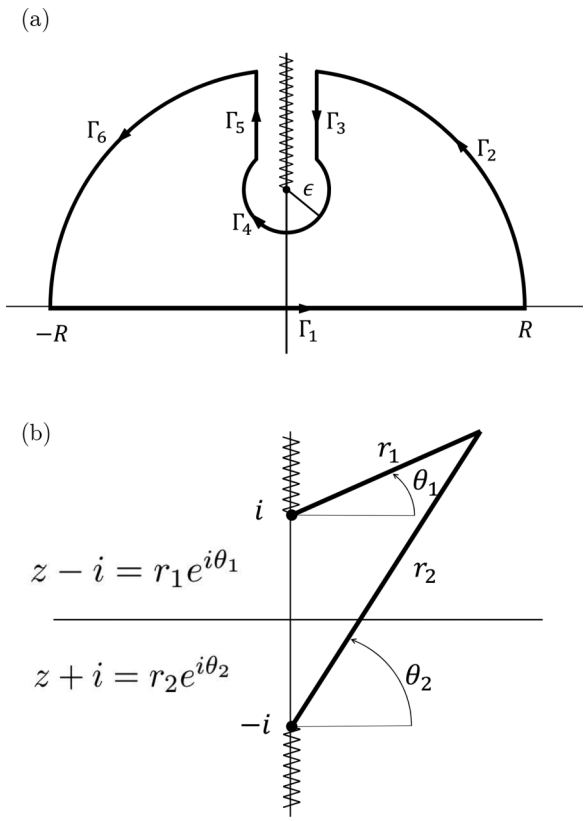

FIG. 5. (a) The contour $\Gamma = \Gamma_1 \cup \Gamma_2 \cup \cdots \cup \Gamma_6$ and (b) the adopted branch cut configuration for the multivalued function $\sqrt{z^2+1}$ for the evaluation of the integral $\int_\Gamma \frac{e^{iz\alpha}}{\sqrt{z^2+1}-\beta} dz$. Note that $-\frac{3\pi}{2} < \theta_1 < \frac{\pi}{2}$ and $-\frac{\pi}{2} < \theta_2 < \frac{3\pi}{2}$.

For example,

$$\begin{aligned}
&\int_{-\infty}^{\infty} \frac{e^{ik_x(x-x')}}{\omega_{\mathbf{k}}(\mu B_1 - \omega_{\mathbf{k}})} dk_x \\
&= \int_{-\infty}^{\infty} \frac{e^{ik_x(x-x')}}{\mu B_1 \omega_{\mathbf{k}}} dk_x + \int_{-\infty}^{\infty} \frac{e^{ik_x(x-x')}}{\mu B_1(\mu B_1 - \omega_{\mathbf{k}})} dk_x \\
&= \frac{1}{\mu B_1 c} \int_{-\infty}^{\infty} e^{i\frac{k}{c}(x-x')\Omega_{m,m'}} \\
&\quad \times \left[\frac{1}{\sqrt{k^2+1}} - \frac{1}{\sqrt{k^2+1} - \frac{\mu B_1}{\Omega_{m,m'}}} \right] dk \\
&= \frac{1}{\mu B_1 c} \left[E_1\left(\frac{|x-x'|\Omega_{m,m'}}{c} \right) \right. \\
&\quad \left. - E_2\left(\frac{|x-x'|\Omega_{m,m'}}{c}, \frac{\mu B_1}{\Omega_{m,m'}} \right) \right].
\end{aligned} \tag{C8}$$

As another example,

$$\begin{aligned}
&\int_{-\infty}^{\infty} \frac{\omega_{\mathbf{k}} e^{ik_x(x-x')}}{\mu B_1 - \omega_{\mathbf{k}}} dk_x \\
&= -\int_{-\infty}^{\infty} e^{ik_x(x-x')} dk_x + \int_{-\infty}^{\infty} \frac{\mu B_1 e^{ik_x(x-x')}}{\mu B_1 - \omega_{\mathbf{k}}} dk_x \\
&= -2\pi\delta(x-x') - \frac{\mu B_1}{c} E_2\left(\frac{|x-x'|\Omega_{m,m'}}{c}, \frac{\mu B_1}{\Omega_{m,m'}} \right).
\end{aligned} \tag{C9}$$

However, the position of neigboring magnetic spheres is distinct, i.e., $x - x' \neq 0$ and thus here $\delta(x-x') = 0$.

[1] B. Zare Rameshti, S. V. Kusminskiy, J. A. Haigh, K. Usami, D. Lachance-Quirion, Y. Nakamura, C.-M. Hu, H. X. Tang, G. E. Bauer, and Y. M. Blanter, Phys. Rep. **979**, 1 (2022).

[2] D. Lachance-Quirion, Y. Tabuchi, A. Gloppe, K. Usami, and Y. Nakamura, Appl. Phys. Express **12**, 070101 (2019).

[3] Y. Li, W. Zhang, V. Tyberkevych, W.-K. Kwok, A. Hoffmann, and V. Novosad, J. Appl. Phys. **128**, 130902 (2020).

[4] D. D. Awschalom, C. H. R. Du, R. He, J. Heremans, A. Hoffmann, J. Hou, H. Kurebayashi, Y. Li, L. Liu, V. Novosad, J. Sklenar, S. Sullivan, D. Sun, H. Tang, V. Tyberkevych, C. Trevillian, A. W. Tsen, L. Weiss, W. Zhang, X. Zhang *et al.*, IEEE Trans. Quantum Eng. **2**, 1 (2021).

[5] H. Huebl, C. W. Zollitsch, J. Lotze, F. Hocke, M. Greifenstein, A. Marx, R. Gross, and S. T. B. Goennenwein, Phys. Rev. Lett. **111**, 127003 (2013).

[6] Y. Tabuchi, S. Ishino, T. Ishikawa, R. Yamazaki, K. Usami, and Y. Nakamura, Phys. Rev. Lett. **113**, 083603 (2014).

[7] X. Zhang, C.-L. Zou, L. Jiang, and H. X. Tang, Phys. Rev. Lett. **113**, 156401 (2014).

[8] Y. Cao, P. Yan, H. Huebl, S. T. B. Goennenwein, and G. E. W. Bauer, Phys. Rev. B **91**, 094423 (2015).

[9] B. Zare Rameshti, Y. Cao, and G. E. W. Bauer, Phys. Rev. B **91**, 214430 (2015).

[10] Y. Tabuchi, S. Ishino, A. Noguchi, T. Ishikawa, R. Yamazaki, K. Usami, and Y. Nakamura, Science **349**, 405 (2015).

[11] X. Zhang, C.-L. Zou, N. Zhu, F. Marquardt, L. Jiang, and H. X. Tang, Nat. Commun. **6**, 8914 (2015).

[12] B. Zare Rameshti and G. E. W. Bauer, Phys. Rev. B **97**, 014419 (2018).

[13] T. Yu, Y.-X. Zhang, S. Sharma, X. Zhang, Y. M. Blanter, and G. E. W. Bauer, Phys. Rev. Lett. **124**, 107202 (2020).

[14] T. Yu, X. Zhang, S. Sharma, Y. M. Blanter, and G. E. W. Bauer, Phys. Rev. B **101**, 094414 (2020).

[15] F. D. M. Haldane and S. Raghu, Phys. Rev. Lett. **100**, 013904 (2008).

[16] Z. Wang, Y. Chong, J. D. Joannopoulos, and M. Soljačić, Nature (London) **461**, 772 (2009).

[17] C.-E. Bardyn, T. Karzig, G. Refael, and T. C. H. Liew, Phys. Rev. B **91**, 161413(R) (2015).

[18] T. Karzig, C.-E. Bardyn, N. H. Lindner, and G. Refael, Phys. Rev. X **5**, 031001 (2015).

[19] A. V. Nalitov, D. D. Solnyshkov, and G. Malpuech, Phys. Rev. Lett. **114**, 116401 (2015).

[20] K. Yi and T. Karzig, Phys. Rev. B **93**, 104303 (2016).

[21] D. Jin, L. Lu, Z. Wang, C. Fang, J. D. Joannopoulos, M. Soljačić, L. Fu, and N. X. Fang, Nat. Commun. **7**, 13486 (2016).

[22] A. Kavokin, G. Malpuech, and M. Glazov, Phys. Rev. Lett. **95**, 136601 (2005).

[23] C. Leyder, M. Romanelli, J. P. Karr, E. Giacobino, T. C. H. Liew, M. M. Glazov, A. V. Kavokin, G. Malpuech, and A. Bramati, Nat. Phys. **3**, 628 (2007).

[24] M. Hafezi, S. Mittal, J. Fan, A. Migdall, and J. M. Taylor, Nat. Photonics **7**, 1001 (2013).

[25] S. Mittal, J. Fan, S. Faez, A. Migdall, J. M. Taylor, and M. Hafezi, Phys. Rev. Lett. **113**, 087403 (2014).

[26] K. Y. Bliokh, D. Smirnova, and F. Nori, Science **348**, 1448 (2015).

[27] T. Ma, A. B. Khanikaev, S. H. Mousavi, and G. Shvets, Phys. Rev. Lett. **114**, 127401 (2015).

[28] T. V. Mechelen and Z. Jacob, Optica **3**, 118 (2016).

[29] X. Cheng, C. Jouvaud, X. Ni, S. H. Mousavi, A. Z. Genack, and A. B. Khanikaev, Nat. Mater. **15**, 542 (2016).

[30] K. Lai, T. Ma, X. Bo, S. Anlage, and G. Shvets, Sci. Rep. **6**, 28453 (2016).

[31] B. Xiao, K. Lai, Y. Yu, T. Ma, G. Shvets, and S. M. Anlage, Phys. Rev. B **94**, 195427 (2016).

[32] A. L. C. Hayward, A. M. Martin, and A. D. Greentree, Phys. Rev. Lett. **108**, 223602 (2012).

[33] K. Fang, Z. Yu, and S. Fan, Nat. Photonics **6**, 782 (2012).

[34] Q. Lin and S. Fan, New J. Phys. **17**, 075008 (2015).

[35] M. Minkov and V. Savona, Optica **3**, 200 (2016).

[36] W. P. Su, J. R. Schrieffer, and A. J. Heeger, Phys. Rev. Lett. **42**, 1698 (1979).

[37] N. Malkova, I. Hromada, X. Wang, G. Bryant, and Z. Chen, Opt. Lett. **34**, 1633 (2009).

[38] V. Yannopapas, Int. J. Mod. Phys. B **28**, 1441006 (2013).

[39] H. Schomerus, Opt. Lett. **38**, 1912 (2013).

[40] M. Xiao, Z. Q. Zhang, and C. T. Chan, Phys. Rev. X **4**, 021017 (2014).

[41] W. Tan, Y. Sun, H. Chen, and S.-Q. Shen, Sci. Rep. **4**, 3842 (2014).

[42] A. P. Slobozhanyuk, A. N. Poddubny, A. E. Miroshnichenko, P. A. Belov, and Y. S. Kivshar, Phys. Rev. Lett. **114**, 123901 (2015).

[43] A. P. Slobozhanyuk, A. N. Poddubny, I. S. Sinev, A. K. Samusev, Y. F. Yu, A. I. Kuznetsov, A. E. Miroshnichenko, and Y. S. Kivshar, Laser Photon. Rev. **10**, 656 (2016).

[44] S. Kruk, A. Slobozhanyuk, D. Denkova, A. Poddubny, I. Kravchenko, A. Miroshnichenko, D. Neshev, and Y. Kivshar, Small **13**, 1603190 (2017).

[45] A. Poddubny, A. Miroshnichenko, A. Slobozhanyuk, and Y. Kivshar, ACS Photonics **1**, 101 (2014).

[46] C. W. Ling, M. Xiao, C. T. Chan, S. F. Yu, and K. H. Fung, Opt. Express **23**, 2021 (2015).

[47] I. S. Sinev, I. S. Mukhin, A. P. Slobozhanyuk, A. N. Poddubny, A. E. Miroshnichenko, A. K. Samusev, and Y. S. Kivshar, Nanoscale **7**, 11904 (2015).

[48] C. A. Downing and G. Weick, Phys. Rev. B **95**, 125426 (2017).

[49] S. R. Pocock, X. Xiao, P. A. Huidobro, and V. Giannini, ACS Photonics **5**, 2271 (2018).

[50] R. Keil, J. M. Zeuner, F. Dreisow, M. Heinrich, A. Tünnermann, S. Nolte, and A. Szameit, Nat. Commun. **4**, 1368 (2013).

[51] E. Saei Ghareh Naz, I. C. Fulga, L. Ma, O. G. Schmidt, and J. van den Brink, Phys. Rev. A **98**, 033830 (2018).

[52] F. Bleckmann, Z. Cherpakova, S. Linden, and A. Alberti, Phys. Rev. B **96**, 045417 (2017).

[53] Z. Fedorova (Cherpakova), C. Jörg, C. Dauer, F. Letscher, M. Fleischhauer, S. Eggert, S. Linden, and G. von Freymann, Light Sci. Appl. **8**, 63 (2019).

[54] D. D. Solnyshkov, A. V. Nalitov, and G. Malpuech, Phys. Rev. Lett. **116**, 046402 (2016).

[55] P. St-Jean, V. Goblot, E. Galopin, A. Lemaître, T. Ozawa, L. L. Gratiet, I. Sagnes, J. Bloch, and A. Amo, Nat. Photonics **11**, 651 (2017).

[56] M. Atala, M. Aidelsburger, J. T. Barreiro, D. Abanin, T. Kitagawa, E. Demler, and I. Bloch, Nat. Phys. **9**, 795 (2013).

[57] M. Xiao, G. Ma, Z. Yang, P. Sheng, Z. Q. Zhang, and C. T. Chan, Nat. Phys. **11**, 240 (2015).

[58] X. Li, Y. Meng, X. Wu, S. Yan, Y. Huang, S. Wang, and W. Wen, Appl. Phys. Lett. **113**, 203501 (2018).

[59] F. Pirmoradian, B. Zare Rameshti, M. F. Miri, and S. Saeidian, Phys. Rev. B **98**, 224409 (2018).

[60] I. S. Jacobs and C. P. Bean, Phys. Rev. **100**, 1060 (1955).

[61] R. Arias and D. L. Mills, Phys. Rev. B **70**, 104425 (2004).

[62] N. A. Pike and D. Stroud, Eur. Phys. J. B **90**, 59 (2017).

[63] J. Zak, Phys. Rev. Lett. **62**, 2747 (1989).

[64] S. Mieszczak and J. W. Kłos, Sci. Rep. **12**, 11335 (2022).

[65] M. Malki and G. S. Uhrig, Europhys. Lett. **127**, 27001 (2019).

[66] M. Malki, L. Müller, and G. S. Uhrig, Phys. Rev. Res. **1**, 033197 (2019).

[67] B. Pérez-González, M. Bello, Á. Gómez-León, and G. Platero, Phys. Rev. B **99**, 035146 (2019).

[68] C. A. Downing, T. J. Sturges, G. Weick, M. Stobińska, and L. Martín-Moreno, Phys. Rev. Lett. **123**, 217401 (2019).